Energy Absorption and Damage Analysis of Glass Fibre Reinforced Polymer Spherical Core Sandwich Structures

Venugopal PANDYARAJ [1]*, Arunachalam RAJADURAI [2], Kani KALAICHELVAN [3]

[1] *Department of Mechanical and Automation Engineering, Sri Sai Ram Engineering College, Chennai-44, India*
[2] *Department of Production Technology, MIT Campus, Anna University, Chennai-44, India*
[3] *Department of Ceramic Technology, AC Tech Campus, Anna University, Chennai-25, India*

http://doi.org/10.5755/j02.ms.38052

Received 29 July 2024; accepted 4 November 2024

The present study describes the energy absorption and damage analysis of the spherical core sandwich structures (SCSS) fabricated using woven Glass Fibre Reinforced Plastic (GFRP) by hand- layup method. Based on the core orientation, the spherical cores are categorized as stagger (S), regular (R), inverted (I), and interlock (L). The pitch distance and diameter of the models considered for the study are 24 mm and 16 mm, respectively. The specimens are subjected to a low velocity impact test (LVIT) at three different energy levels 9.9, 27.5, and 53.9 J respectively. Evaluations are carried out on the different kind of parameters namely coefficient of restitution (COR),energy absorption ratio, and energy loss percentage maximum displacement, maximum force, absorbed energy, and rebound energy. Among the models at every impact velocity it is found that the model R sustains a maximum force of 3078 N at 7 m/s impact velocity. The stagger model has recorded a maximum displacement of 34.4 mm among all velocities, whereas the regular model reveals a minimum displacement of 4.9 mm based on the analysis of maximum displacement. Similarly, the regular model has a maximum energy absorption ratio at 5 and 7 m/s respectively, whereas at 3 m/s the interlock model absorbs more energy. The failure pattern of the specimens is analyzed through visual inspection and ultrasound testing. Matrix cracking and fibre breakage are the typical failures seen in the model at 3 m/s, while core crushing and perforation are seen at 5 and 7 m/s impact velocities. The damage area is minimum for the interlock model whereas it is maximum for the stagger model.

Keywords: GFRP, sandwich structures, impact test, spherical, composite materials.

1. INTRODUCTION

Thin facing sheets are used to build sandwich structures, and they are attached at the top and bottom of the lightweight core with resin. The low velocity impact test was used to examine the sandwich structures' energy-absorbing properties. Rajesh Mathivanan and Jerald (2010) [1] investigated the impact response of Glass Fiber Reinforced Polymers (GFRP) laminates subjected to low velocity impact test at velocity 2 to 4.5 m/s and found that the elastic property of the fibre materials enhance the dynamic properties of the sandwich structures. In glass epoxy laminates, two failure modes were noted: perforation and crack initiation. The GFRP laminate exhibited delamination at 3.1 m/s, whereas at 4.4 m/s it underwent complete perforation of the structures. Antony Arul Prakash et al. (2014) [2] studied the impact response and the impact of cell size of honeycomb sandwich constructions composed of GFRP employing vacuum bag moulding techniques. The core sections' various cell sizes were 8, 12, 16, and 20 mm. The impact energies used in the trials ranged from 7 J to 50 J, respectively. The load vs. time and energy vs. time graphs were employed to investigate the damage process and energy absorption. The findings showed that the 8 mm cell had the highest peak load, the smallest amount of deflection, and the most effective damage resistance. It was additionally observed that the load-bearing capability drops with increasing cell size.

The specimens typically exhibited matrix cracking, fiber breakage, top facing sheet failure, core crushing, and debonding of the bottom facing sheet from the core as a series of failures.

CesimAtas et al. (2015) [3] investigated how the thickness of the face sheet affected the way foam core sandwich structures responded to impacts. The resin infusion procedure with vacuum assistance was used to create the specimens. The specimens of size $100 \times 100 \times 16$ mm were subjected to a hemispherical impactor of diameter 12.7 mm and mass 5 kg. The impact energy ranged from 5 J to 50 J. It was found that as the facing sheet thickness increased the perforation threshold increased in a linear fashion. The common damage modes seen were fractures of fibres at the top and bottom skins, delaminations between the facing sheet and core, and core shear fractures. Sun Ying et al. (2016) [4] studied the impact response of carbon- aramide/epoxy hybrid composites as per ASTM D 7136. The specimens were fabricated by resin transfer moulding method and were subjected to a drop test having a spherical impactor of mass 6.5 kg and diameter 12.7 mm respectively. The size of the specimen taken for study was $150 \times 100 \times 4$ mm. The damage areas were analysed using ultrasound c-scan. The common damages found in the tested laminates were matrix cracking, buckling delamination between the piles, and fibre breakage.

* Corresponding author: V. Pandyaraj
E-mail: *pandyaraj.mu@sairam.edu.in*

Vishwas Mahesh et al (2019) [5] investigated the response of LVI for novel Jute (J)/rubber (R) bio composite laminates. The performance of the composites was evaluated based on peak force, absorption of energy, loss percentage of energy, energy absorption ratio, and coefficient of restitution. The specimens of size 150x 150 mm have undergone LVIT with an impactor of mass 3.5 kg. The impact energy chosen for the studies were 10.24, 23.95, and 37.67 J respectively. The model JRJRJ showed lower damage resistance when compared to other specimens. The majority of the specimens failed due to puncture caused by the tearing mechanism. Further, it was observed that there is no delamination in flexible composites. Bulut (2020) [6] studied the impact response of eco- friendly sandwich structure fabricated using basalt fibre/polypropylene honeycomb core sandwich composites. The influence of facing sheet thickness and energy impact were studied based on the ASTM D7136. The nominal size of the specimen was 80 × 80 × 10 mm. The samples were drop tested by a hemispherical impactor diameter of 12.7 mm with a mass of 5 kg at impact energies of 10, 20, and 30 J, respectively. It has been understood that the maximum load increases with increasing the facing sheet thickness increases by reducing the residual deformations. The duration of the impact was much less at 10 J. The common failures observed in the specimens were fibre breakage, core crushing, and top and bottom facing sheet failure. Pandyaraj and Rajadurai [7 – 9] studied the compression behaviour and flexural behaviour of SCSS. The drop weight test was performed to assess the energy absorbing characteristics of the SCSS fabricated using woven 32 mm pitch distance. In the present study, the absorption of energy and failure pattern analysis of the SCSS subjected to LVIT are carried out in a detailed manner for the models fabricated using 24 mm pitch distance.

2. FABRICATION OF SPECIMEN AND EXPERIMENT METHODOLOGY

The SCSS of four distinct configurations namely R, I , L, and S were made in this study making use of 25 % E-glass fibre reinforced with 75 % vinyl ester (matrix), which was manufactured by hand moulding. The core is made up of two layers of 300 gsm woven E-glass fabric, while the face sheet is made up of a single 600 gsm layer. Fig. 1 shows the fabrication process of the SCSS and Fig. 2 shows the photograph of the fabricated specimens. The experiment methodology was elaborated in detail [9]. The size of the specimen is 110 × 100 mm.

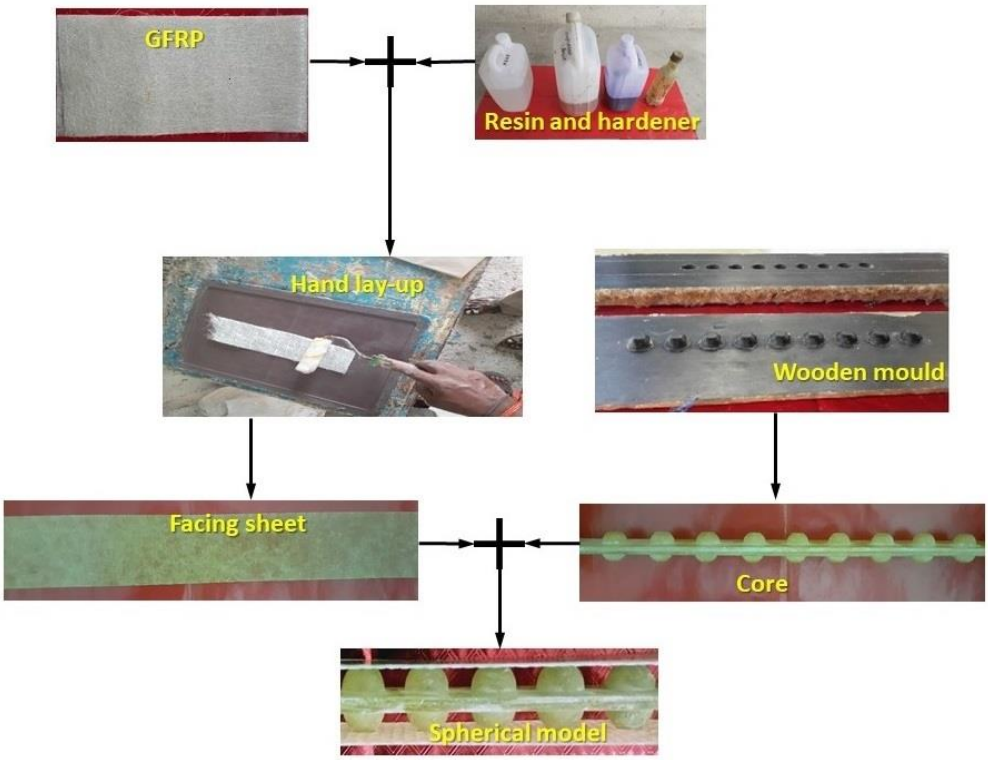

Fig. 1. Fabrication process of the SCSS

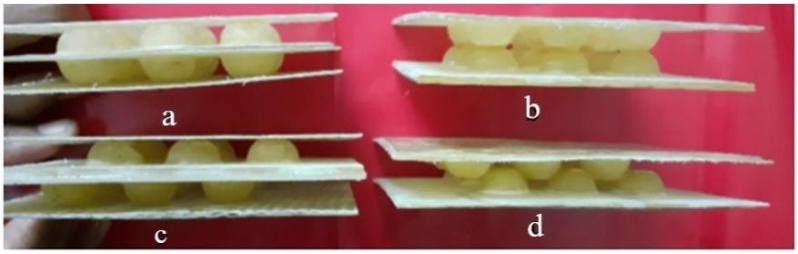

Fig. 2. Photographs of the fabricated specimens: a – regular; b – inverted; c – stager; d – interlock

3. ENERGY VS TIME

From Fig. 3 among woven-GFRP models for 3 m/s, it is found that all the models except (I) show smooth curve patterns.

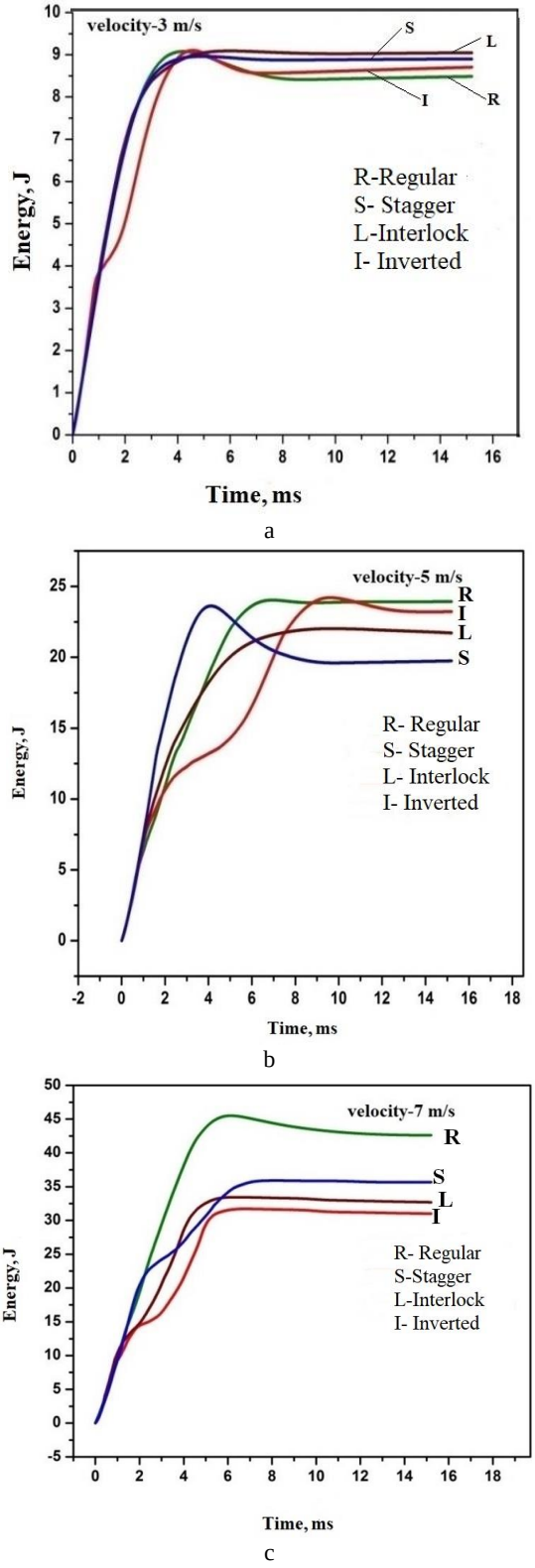

Fig. 3. Energy vs time for impact velocity of: a – 3 m/s; b – 5 m/s; c – 7 m/s

While in the model (I) initially the energy value curve reaches 4 J of energy at 1 milliseconds (ms) of time and gets deflected and then reaches 9 J of energy at 4 ms of time, thus showing a deflected curve pattern. The model absorbs 8.6 J of energy, while the rebound energy is 0.7 J.

Whereas for the remaining models R, L and S the energy absorbed is 8.4, 8.8, and 8.5 J. Similarly the rebound energy of the models are as follows 0.8, 0.2, and 0.4 J. It has determined that the model L absorbs more energy with a value of 8.8 J with less rebound energy. Similar patterns are observed in 5 and 7 m/s impact velocities of SCSS. The concept of COR, ratio for energy absorption and ELP are discussed in detail [9].

4. DAMAGE ANALYSIS

Four distinct configurations of SCSS are subjected to LVIT at 3, 5, and 7 m/s and the results are summarized in Table 1.

Table 1. The absorbed energy values for woven-GFRP sandwich models

Model	Energy absorbed, J	Energy absorption ratio, Ea/Ei	Elastic energy, J	COR	ELP
3 m/s					
R	8.4	84.50	0.8	0.28	92.16
I	8.6	86.86	0.7	0.26	93.24
L	8.8	88.88	0.2	0.14	98.04
S	8.5	85.85	0.4	0.20	96.00
5 m/s					
R	23.7	86.18	0.3	0.10	99.00
I	22.5	81.81	1.6	0.24	94.24
L	20.5	74.54	0.1	0.06	99.64
S	18.5	67.27	5.3	0.43	81.51
7 m/s					
R	43.0	79.77	2.1	0.19	96.39
I	31.0	57.50	0.0	0.00	100.00
L	32.0	59.36	0.8	0.12	98.56
S	37.0	68.64	0.0	0.00	100.00

Fig. 4 shows the typical photograph of the force vs. time curve showing peaks corresponding to damages.

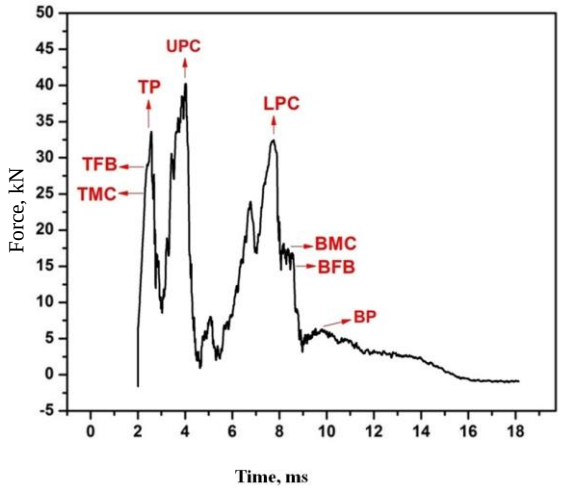

Fig. 4. Force vs time showing peaks corresponding damages

The damages observed in the SCSS are categorized as matrix cracking in the top face sheet (TMC), Top fibre breakage (TFB) and perforation in the top face sheet (TP).

Similar failures are noticed in the bottom facing sheet and are categorized as matrix cracking in the bottom facing sheet (BMC), Bottom fibre breakage (BFB) and perforation in the bottom facing sheet (BP). The damages observed in the core region are upper and lower portion of the core crushing namely (UPC and LPC). The crack propagation progress and the defects in the model could be assessed and cross-verified by visual inspection as well as ultrasound testing. The damage area is further characterized as Top damage area (TDA), Top fracture area (TFA), Bottom damage area (BDA), and Bottom fracture area (BFA).

The damage areas of the SCSS are tabulated in Table 2.

Table 2. Damage area values of SCSS

Model	Depth of penetration, mm	Max. force, N	Top side		Bottom side	
			TDA	TFA	BDA	BFA
			mm^2			
3 m/s						
R	NIL	1682	3200	150	NIL	NIL
I	3	2021	2350	400	NIL	NIL
L	8	1796	1400	132	NIL	NIL
S	NIL	1693	3950	NIL	NIL	NIL
5 m/s						
R	8	1948	3400	500	225	NIL
I	14	1986	2840	460	1800	NIL
L	14	1944	2000	480	3160	440
S	9	2967	4225	250	NIL	NIL
7 m/s						
R	18	3078	3600	2800	2376	1224
I	20	2501	2125	895	2100	694
L	15	2291	1425	721	3575	697
S	20	2372	3625	1912	3450	655

5. FAILURE INSPECTION

The common failures observed in the SCSS when it is subjected to impact load are dent, matrix cracking, fibre breakage, perforation of the face sheet, crushing of core and debonding of facing sheet and core. The damage is assessed using the top lighting techniques and ultrasound testing. The various features observed in the tested specimen are classified into the following nomenclature.

Nomenclature

Dent	Shallow deformation in the surface of the specimen
Matrix cracks	It is a short or long crack in the facing sheet
Fibre breakage	Broken fibre observed on the facing sheet
Perforation	Complete penetration of the impactor on the facing sheet
Debonding	Separation of facing sheet and core
Core failure	Damage of the core such as crushing and perforation in the core

5.1. Failure pattern of top face sheet

The face sheet failure at the top is noticed to exhibit various patterns of failures in all the models at various velocities as shown in Fig. 5. A dent or depression associated with the matrix cracking is observed in every model at 3 m/s velocity. Whereas at 5 m/s the matrix cracking observed in the models is circular and in addition to it splits or cracks originate from the damaged area due to fibre breakage. At 7 m/s the damages seen in the specimens R and S are irregular in shape with a lot of branched cracks. Whereas for the remaining models the damaged area is circular in shape with the combination of fibre breakage. In addition to it in the model R and S the face sheet is fully debonded from the core. Similar type of damage patterns are noticed in the honeycomb sandwich constructions (Antony Arul Prakash et. al. 2014) [2].

Fig. 5. a – top damage portion of the SCSS; b – typical photograph of the top side of R at 7 m/s impact velocity

5.2. Failure pattern of core

Fig. 6 shows the core portion of SCSS. At 3 m/s velocity, there is no significant damage in the core region for all the specimens. Whereas at 5 m/s, the spheres in the upper side of the core get partially crushed for the majority of the model, while in I and L the lower part of core also gets damaged. Similarly, at 7 m/s all the models exhibit failures in the lower part of the core and the sphere is partially or completely crushed. In model R the sphere in the upper part of the core is crushed and falls off. Whereas in model L the core split into two halves which could be correlated to the partial locking of spheres between each other.

5.3. Failure pattern of bottom face sheet

The failure noticed in the bottom face sheet of the specimens for all velocities is shown in Fig. 7. At 3 m/s the specimen doesn't exhibit any damage.

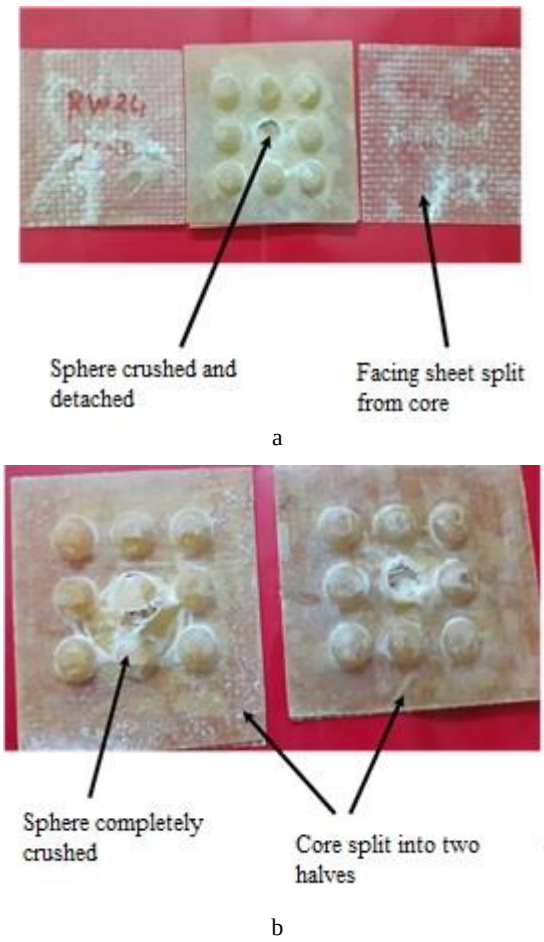

Fig. 6. Photographs of core portion: a – regular; b – interlock model

While at 5 m/s velocity the matrix cracking observed in the models is circular in shape with the combination of cracks. At 7 m/s velocity, majority of the model exhibits a combination of fibre breakage and cracks along with circular shape damage. In addition to it in model I the detachment of the bottom face sheet and core is noticed.

5.4. Damage area analysis

A detailed assessment of the extent of damage of the SCSS was carried out using visual inspection and ultrasound inspection. The damaged areas have been categorised as Top damage area (TDA), Top fracture area (TFA), Bottom damage area (BDA) and Bottom fracture area (BFA). Wherein, damage area (DA) refers to the area where matrix cracking alone has occurred and fracture area refers to the area wherein fibre breakage has also occured. In addition to it, the penetration depth is estimated by a dial gauge. From Table 2 among woven-GFRP spherical models at 3 m/s velocity, it is found that the damage area is maximum for S whose value is 3950 mm^2, which indicates that 35.0 % of the specimen had been damaged. Whereas the specimen L has a minimum value of 1400 mm^2 (12.7 %). While comparing among 5 m/s it is found that model S shows maximum damage area of 4225 mm^2, which indicates 38.4 % of the damage.

Whereas the model L shows the minimum damage area of 2000 mm^2 (18.18 %). Among 7 m/s velocity the specimen S shows a maximum damage area of 3625 mm^2 which implies the contribution of 32.9 % of the damage, whereas the model L shows the minimum damage area of 1425 mm^2 (12.9 %).

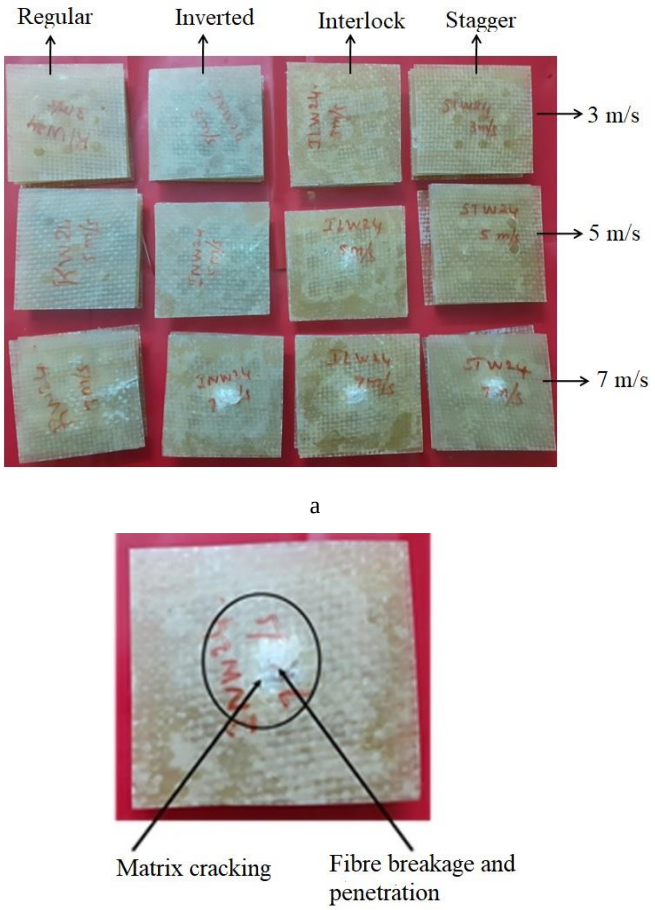

Fig. 7. a – bottom damage portion of the SCSS; b – typical photograph of the bottom side of I at 7 m/s impact velocity

From Table 2 among woven-GFRP spherical models at 3 m/s it is found that fracture area is maximum for I with a value of 400 mm^2 (3.63 %), whereas model S shows no fracture area. While comparing among 5 m/s velocity it is noticed that the specimen R shows the maximum fracture area of 500 mm^2 (4.5 %), whereas model S shows the minimum fracture area of 250 mm^2 (2.27 %). Among 7 m/s specimen R shows the maximum fracture area of 2800 mm^2 (25.45 %), whereas model L shows the minimum fracture area of 721 mm^2 (6.55 %).

From Table 2 among woven-GFRP spherical specimens at 3 m/s it is noticed that there is no damaged area on the bottom side. While comparing among 5 m/s it is found that model L shows the maximum bottom damage area of 3160 mm^2 (28.7 % of damages), whereas the model S shows no bottom damage area. Among 7 m/s specimen L shows the maximum bottom damage area of 3575 mm^2 (32.5 %), whereas the model I shows the minimum bottom damage area of 2100 mm^2 (19.09 %). From Table 2 at 3 m/s velocity, it is noticed that there is no bottom fracture area in the models. While comparing among 5 m/s it is seen that model L shows the maximum bottom fracture area of 440 mm^2 (4 %), whereas the remaining models

show no bottom fracture area. Among 7 m/s specimen R shows the maximum bottom fracture area of 1224 mm^2 (11.12 %), whereas model S shows the minimum bottom damage area of 655 mm^2 (5.9 %). As the impactor hits the specimen the top facing sheet absorbs more amount of energy when compared to the bottom facing sheet. While the impactor starts to descend the energy is dissipated, which results in the minimum absorption by the bottom facing sheet [9]. So the maximum damages are noticed in the top facing sheet than the bottom. But while comparing fracture area it is noted that fibre breakage occurs near the area where the impactor penetrates the specimen. This is the reason for the value of fracture area to differ minimum among top and bottom facing sheets while comparing among damage area. Similarly from Table 2 at 3 m/s velocity, it is found that penetration depth is maximum for the model L with a value of 8 mm, whereas the models R and S show no penetration. While comparing among 5 m/s it is noted that the depth is maximum for the model L and I with a value of 14 mm, while model R shows an 8 mm depth of penetration. Among 7 m/s velocity model I show the maximum depth of penetration with a value of 20 mm. Fig. 8 shows the graphs of the top damage area, bottom damage area, top fracture area, and bottom fracture area of spherical core sandwich structures.

5.5. Ultrasound testing

The tested specimens are subjected to ultra sound testing in order to assess the damage area both at the top and bottom surface of sandwich constructions. Fig. 9 shows the typical photographs of the ultrasound c- scan images of the top surface of the regular model and inverted model. The vertical colour bar ranges from white to red which is measured as 0 to 100. The transmitted signal from the probe is received at the receiver end without any scattered then that particular region is represented in red colour which indicates that there is no damage.

If the area is indicated by white colour then it indicates all the signals are lost and there is perforation in that particular area [9]. The remaining colour bar indicates the matrix cracking and fibre breakages as per the signals received at the receiver end.

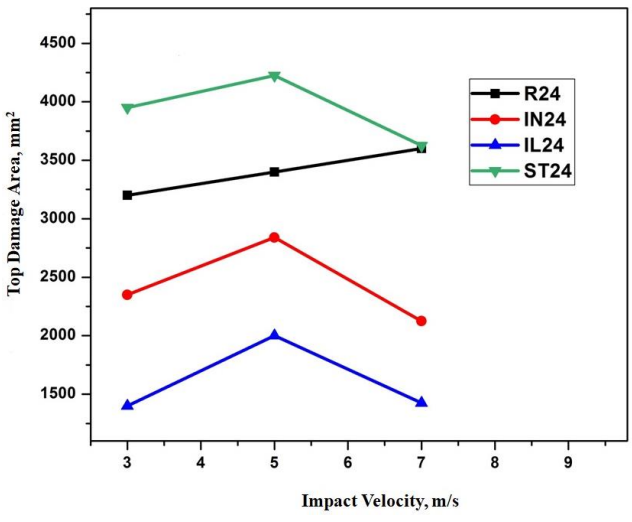

a

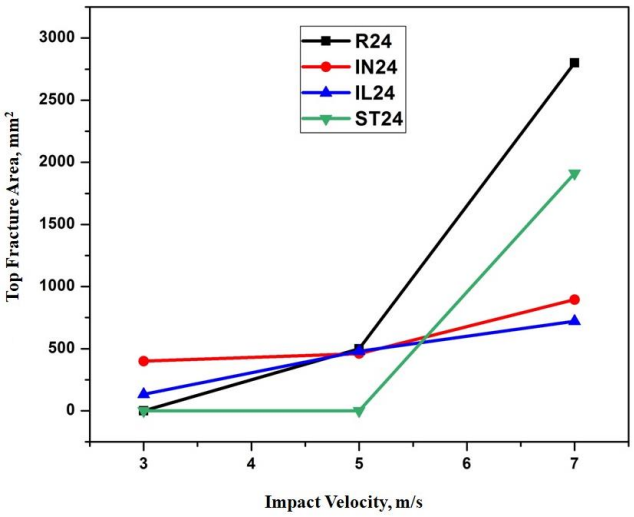

b

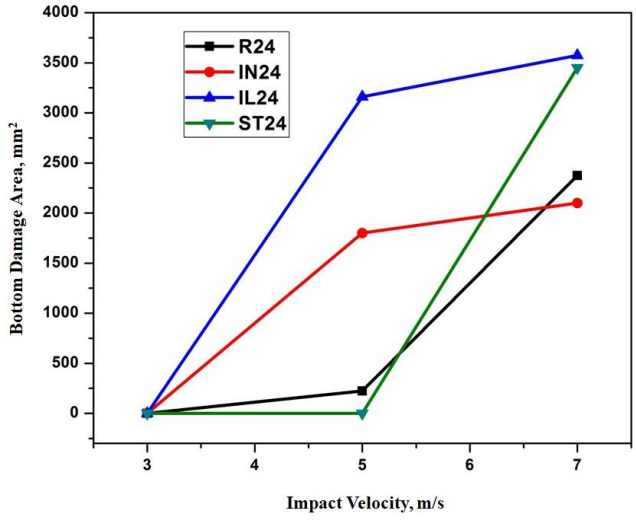

c

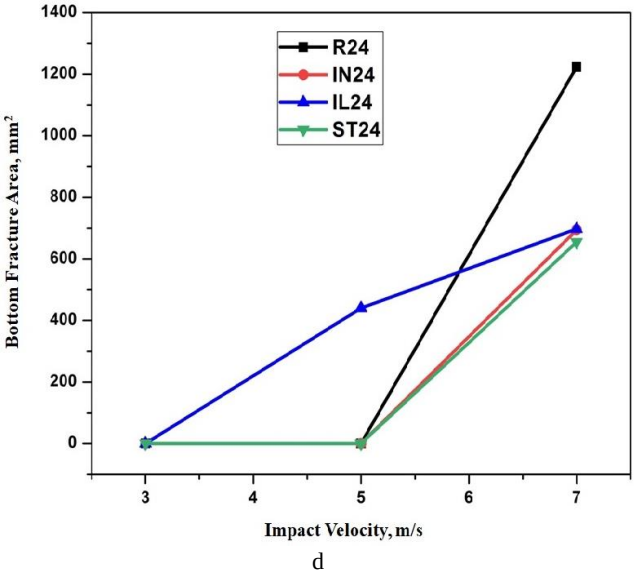

d

Fig. 8. Damage area: a – top; b – bottom; Fracture area: c – top; d – bottom fracture area

6. CONCLUSIONS

The SCSS namely regular, inverted, interlock, and stagger are fabricated using woven GFRP and are tested using LVIT at 3, 5, and 7 m/s respectively.

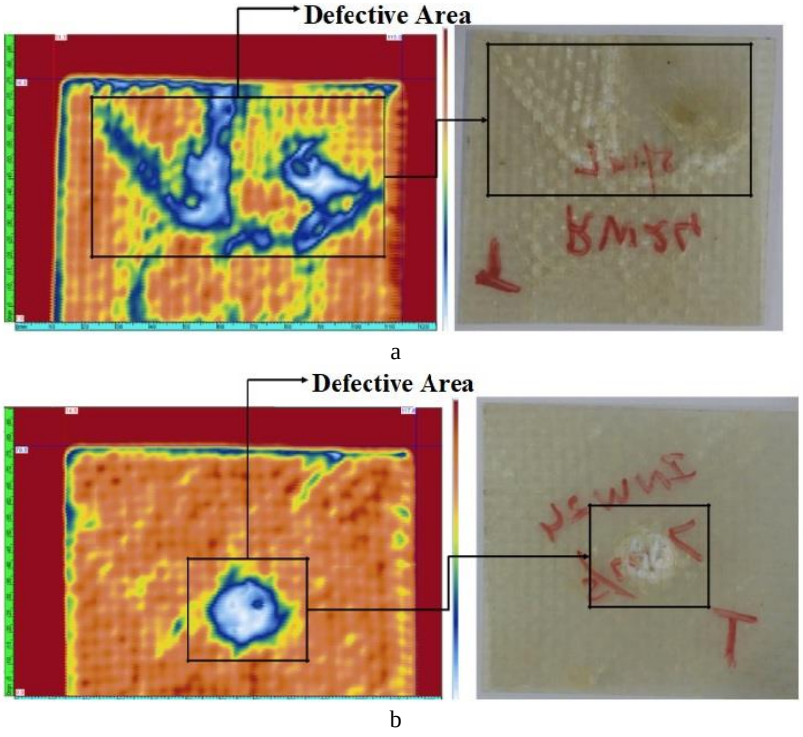

Fig. 9. Typical photographs of the ultrasound images of the models: a – regular; b – inverted

The absorption of energy is higher for interlock at 3 m/s while at 5 and 7 m/s impact velocity the specimen R absorbs more energy because the structure is rigid in the middle and the spheres are closely packed to each other. The damaged areas of the tested specimens are assessed by visual inspection and ultrasound testing. It is found that as the velocity increases all the models exhibit maximum damages. The typical failures noticed in the specimens at 3 m/s are matrix cracking and fibre breakage, whereas, at 5 m/s core crushing is seen. However, at 7 m/s impact velocity, perforation of the specimens is also seen in I and S models. The SCSS can be used for light load applications such as partition walls and roof tops.

REFERENCES

1. **Rajesh Mathivanan, N., Jerald, J.** Experimental Investigation of Woven E-glass Epoxy Composite Laminates Subjected to Low Velocity Impact Test at Different Levels *Journal of Minerals & Material characterization & Engineering* 9 (7) 2010: pp. 643 – 652. https://doi.org/10.4236/jmmce.2010.97046
2. **Prakash, A.A., Mohan, B., Rajadurai, A., Jaswin, A.** Low Velocity Impact Behaviour of Glass Fabric/Epoxy Honeycomb Core Sandwich Composites *Science and Engineering of Composite Materials* 22 (5) 2015: pp. 525 – 538. https://doi.org/10.1515/secm-2013-0069
3. **Cesim, A., Umut, P.** The Effect of Face Sheet Thickness on Low Velocity Impact Response of Sandwich Composite with Foam Cores *Journal of Sandwich Structures and Materials* 2015: pp. 1 – 14. https://doi.org/10.1177/1099636215613775
4. **Sun, Y., Tang, M., Rong, Z., Shi, B., Chen, Li.** An Experimental Investigation on the Low Velocity Impact Response of Carbon-Aramide/Epoxy Hybrid Composite Laminates *Journal of Reinforced Plastics and Composites* 2016: pp. 1 – 13. https://doi.org/10.1177/0731684416680893
5. **Mahesh, V., Joladarashi, S., Kulkarni, S.M.** An Experimental Investigation on Low-Velocity Impact Response of Novel Jute/Rubber Flexible Bio-Composite *Composite Structures* 225 2019: pp. 111190. https://doi.org/10.1016/j.compstruct.2019.111190
6. **Bulut, M.** Low-velocity Impact Tests on Basalt Fiber/Polypropylene Core Honeycomb Sandwich Composites *Mechanics of Composite Materials* 56 (1) 2020: pp. 121 – 130. https://doi.org/10.1007/s11029-020-09866-6
7. **Pandyaraj, V., Rajadurai, A.** Experimental Investigation of Compression Strength in Novel Sandwich Structure *Material Today Proceedings* 5 2018: pp. 8625 – 8630. https://doi.org/10.1016/j.matpr.2017.11.561
8. **Pandyaraj, V., Rajadurai, A.** Experimental Investigation on Flexural Behaviour of Spherical Core Sandwich Structure *Journal of Reinforced Plastics and Composites* 40 (3 – 4) 2021: pp. 143 – 164. https://doi.org/10.1177/0731684420947801
9. **Pandyaraj, V., Rajadurai, A.** Experimental Investigation on Low-Velocity Impact Response of Spherical Core Sandwich Structure *Journal of Composite Materials* 57 (3) 2023: pp. 425 – 442. https://doi.org/10.1177/00219983221146265